PHYSICAL REVIEW A VOLUME 23, NUMBER 3 MARCH 1981

Theory of quantum-mechanical effects on the thermodynamic properties of Lennard-Jones fluids

Richard A. Young
Department of Physics, University of Arizona, Tucson, Arizona 85721
(Received 15 September 1980)

In this paper we consider the problem of computing the quantum-mechanical corrections to the thermodynamic properties of systems whose two-particle interaction may be described by a Lennard-Jones 6-12 potential. Using a procedure first developed by Feynman, together with physical arguments, we develop an effective two-particle 6-12 potential which includes quantum-mechanical corrections. Using this potential in conjunction with the theory of corresponding states we compute the quantum effects on: (i) the second virial coefficient, (ii) the critical-point location, (iii) the surface tension, (iv) the critical-point amplitudes and exponents, (v) the correction to scaling amplitudes and exponents, (vi) the liquid-gas and solid-liquid phase boundaries, and (vii) the Debye temperature at the melting point. In all cases there is good qualitative and frequently quantitative agreement with experimental results. The theory is limited to "high temperatures" since exchange effects are not included.

I. INTRODUCTION

The influence of quantum-mechanical (QM) effects on the thermodynamic properties of nearly classical liquids is a long-standing question which was first addressed in the pioneering work of de Boer *et al.*[1-3] The approach used by these authors involved the examination of corrections to corresponding-states theory as a function of the dimensionless QM parameter λ ($\lambda = h/\sigma\sqrt{m\epsilon}$, m = mass, and ϵ and σ measure the energy and length scale of the potential energy) for the rare gases. By plotting experimentally obtained values of the reduced critical temperature (kT_c/ϵ), molar volume ($V_c/N\sigma^3$, N = Avogadro's number), and pressure ($P_c\sigma^3/\epsilon$) as a function of λ, it was possible to predict the location of the critical point of ^{3}He. This approach of examining trends in experimental data as a function of λ has also been extended to include the transport properties of the rare gases.[4]

Attempts to compute QM corrections to the thermodynamic properties of simple liquids have met with limited success. In the case of neon ($\lambda = 0.577$), thermodynamic perturbation theory may be used to obtain excellent agreement with experiment.[5] Unfortunately, perturbation theory is sufficiently slowly convergent that this approach is not readily applicable to liquids such as H_2, ^{4}He, and ^{3}He where the values of λ are much larger (Table I). Attempts have been made to avoid power-series expansions in λ through the introduction of model hard-core equations of state.[6,7] While this approach gives good qualitative agreement for the location of the critical point as a function of λ, it suffers from the strange model dependence that one-dimensional hard-core models seem to give better results than three-dimensional models.[8] In addition, it is difficult to apply this method to calculate thermodynamic properties other than the critical-point location. More recently, Nasanow *et al.*[9,10] have computed the zero-temperature properties of quantum liquids for realistic two-body potentials. The methods and results are, however, not generalizable to the case of finite temperatures near the critical point. Thus, in spite of the rather long history of this problem, there is not at present any sufficiently quantitative finite temperature theory which would yield estimates of QM effects on the thermodynamic properties of, e.g., H_2, ^{4}He, and ^{3}He. This question assumes added relevance with recent development of a quantitative theory of critical-point phenomena[11] for classical fluids and the subsequent use of this theory in the interpretation of the results of high precision experiments on ^{3}He near its critical point.[12]

In this paper we present a theory which is capable, in a very algebraically simple manner, of providing a qualitative and frequently quantitative description of the λ dependence of a wide range of thermodynamic properties. All of our results are based on the assumption that the bare two-body Lennard-Jones 6-12 potential may be replaced with a QM corrected Lennard-Jones potential whose parameters are temperature (T) and λ dependent. The theory of corresponding states[13] is then used, in conjunction with the corrected potential, to compute the λ dependence of thermodynamic properties. The theory, quite frankly, lacks the mathematical rigor that we would prefer. However, the approximations which are invoked all have a sound physical basis and the subsequent results often agree remarkably well with the experimental data.

The remainder of the paper is organized as follows: Section II describes our basic approach to the problem and motivates the approximations we shall use. In Sec. III we apply our theory to the calculation of the λ dependence of the second

virial coefficient, critical-point location, and surface tension on the coexistence curve for a number of simple liquids (Table I). Section IV contains an analysis of the λ dependence of the liquid-gas coexistence curve and includes a quantitative estimate of the λ dependence of critical-point exponents, amplitudes, and "corrections-to-scaling" amplitudes and exponents. In Sec. V we apply our theory to the solid-liquid coexistence curve and the Debye temperature of quantum solids near the melting point. Finally in Sec. VI we summarize our results and discuss possible refinements of the theory.

II. THEORETICAL DEVELOPMENT

As mentioned in Sec. I we shall assume, for the materials of interest, that we can consider the atoms or molecules to interact via a Lennard-Jones 6-12 potential given by

$$V(r) = 4\epsilon[(\sigma/r)^{12} - (\sigma/r)^{6}], \tag{2.1}$$

where ϵ and σ are given in Table I.[13-15] While such a potential certainly represents an overly simplified approximation,[16] it does permit a rigorous formulation of a theory of corresponding states using classical statistical mechanics.[13] Thus, if we define a reduced temperature, pressure, and molar volume by

$$T^* = kT/\epsilon, \quad p^* = P\sigma^3/\epsilon, \quad V^* = V/N\sigma^3,$$

where k is Boltzmann's constant, then corresponding-states theory would predict that all the substances listed in Table I would have the same reduced equation of state and thus the same critical-point values T_c^*, P_c^*, and V_c^*. The systematic deviation from constancy of these reduced quantities (Table I) as λ increases is indicative of the increasing influence of QM effects.

Also listed in Table I is the dimensionless quantity $P_c^* V_c^*/T_c^* = P_c V_c/kT_c$, which is much less sensitive to changes in λ. This insensitivity provides a significant motivation for our essential assumption that QM effects may be accounted for by the replacement $\epsilon \to \tilde{\epsilon}(T^*, \lambda)$ and $\sigma \to \tilde{\sigma}(T^*, \lambda)$ in Eq. (2.1), i.e., we shall assume that the major effect of QM corrections is to produce an effective potential of the same form as the bare potential but with temperature and λ-dependent parameters $\tilde{\epsilon}$ and $\tilde{\sigma}$ (hereafter an ~ quantity indicates that QM effects have been included in its evaluation). This assumption guarantees that $P_c^* V_c^*/T_c^*$ is independent of λ which, as seen in Table I, is a rather reasonable approximation. In addition, our approximation allows us the full use of all the results of corresponding-states theory and classical statistical mechanics, i.e., once we have lumped all QM effects in $\tilde{\epsilon}$ and $\tilde{\sigma}$ a system may be considered as classical. The most glaring defect of the above approximation is its inability to include exchange effects; as a result our results become increasingly suspect as $T^* \to 0$. Fortunately, however, there is a significant range of temperatures $\lesssim T_c^*$ where exchange effects are rather unimportant and the theory is capable of yielding meaningful numbers.

To determine the functions $\tilde{\epsilon}$ and $\tilde{\sigma}$ we use the procedure, first developed by Feynman[17] (see Appendix A for an outline), of replacing the bare potential with an effective potential given by

$$\tilde{V}(r) = \left(\frac{\alpha}{\pi}\right)^{3/2} \int V(|\vec{\mathbf{r}}'|) e^{-\alpha|\vec{\mathbf{r}}-\vec{\mathbf{r}}'|^2} d^3\vec{\mathbf{r}}', \tag{2.2}$$

where $\alpha = 3mkT/\hbar^2 = 3(2\pi)^2 T^*/\lambda^2\sigma^2$. This potential contains the QM corrections through the Gaussian average whose width is determined by α. If we attempt direct evaluation of Eq. (2.2) using Eq. (2.1) we find that the integral diverges for all r due to the singular nature of $V(r)$ as $r \to 0$. We can, however, overcome this problem by noticing that in the high-temperature limit ($T \to \infty$) our Gaussian average approaches a Dirac δ function. We would expect in this case to get a good approximation to $\tilde{V}(r)$ for $r \gtrsim \sigma$ by neglecting the divergence generated by the infinity in $V(r)$. For temperatures such that $\alpha\sigma^2 \gtrsim 4$ we would expect that $\tilde{V}(r)$ would be rather insensitive to the behavior of $V(r)$ in the core region as long as $r \gtrsim \sigma$. We therefore choose to expand $V(r)$ as a power series in $|\vec{\mathbf{r}}| - r_0$, where $r_0 = 2^{1/6}\sigma$ is the location of the minimum of $V(r)$. Keeping the first four terms in this series and evaluating (2.2) for $r \approx r_0$ we find that the location of the minimum of $\tilde{V}(r)$ is shifted to $2^{1/6}\tilde{\sigma}$ and the value at the minimum to $-\tilde{\epsilon}$ where

$$\tilde{\epsilon}/\epsilon = 1 - 14.3x^{-1} + 104.9x^{-2}, \tag{2.3}$$

$$\tilde{\sigma}/\sigma = 1 + 3.77x^{-1}, \tag{2.4}$$

and $x = \alpha\sigma^2$. The geometry and length scales involved are illustrated in Fig. 1. An outline of the calculation may be found in the Appendix. In arriving at Eqs. (2.3) and (2.4) we have consistently assumed that $x \gg 1$ and $r \approx r_0$. Since Eq. (2.2) implies that $\tilde{V}(r) \to V(r)$ as $\alpha \to \infty$, we may regard Eqs. (2.3) and (2.4) as the leading terms in an asymptotic series. In the applications to follow it will be necessary to deal with situations where the condition $x \gg 1$ is not satisfied and a modification of Eqs. (2.3) and (2.4) is necessary. A straightforward attempt to include higher powers of x^{-1} is both mathematically cumbersome and of questionable utility. We therefore have chosen to use physical arguments to arrive at reasonable

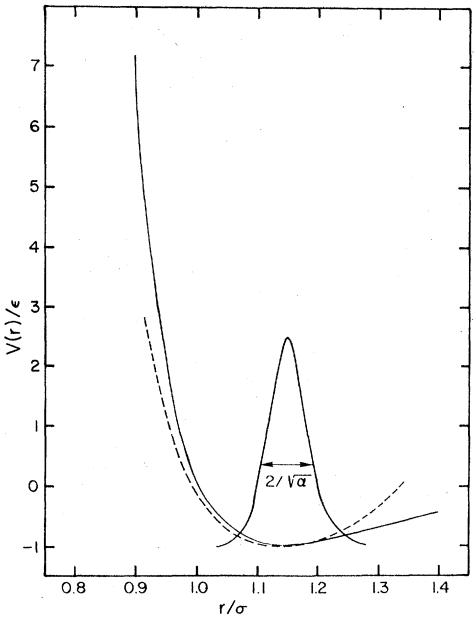

FIG. 1. Normalized Lennard-Jones 6-12 potential, ———, and fourth-order power-series expansion about minimum ----. Also shown is a Gaussian wave packet used to compute the effective potential via Eq. (2.2).

expressions for $\tilde{\epsilon}/\epsilon$ and $\tilde{\sigma}/\sigma$ for $x \lesssim 1$.

Since the expression for $\tilde{V}(r)$ may be regarded as the Gaussian average for a particle of reduced mass $m/2$ moving in a potential $V(r)$, we would expect on physical grounds that the divergence of $\tilde{V}(r)$ would be eliminated by a more exact treatment of the repulsive core region. Such a treatment would presumably involve replacing the "plane-wave" Gaussian wave packet with a Gaussian made up of wave functions which would be excluded from the "hard-core" region. Under these circumstances, due to the short-range nature of $V(r)$, we expect for $\alpha \approx 1/\sigma^2$, i.e., $x \lesssim 1$, that the effective hard core would be given by the radius of the Gaussian plus σ, i.e., $\tilde{\sigma} \approx 1/\sqrt{\alpha} + \sigma \approx 2/\sqrt{\alpha}$ (Fig. 1). Consequently we shall assume $\tilde{\sigma}/\sigma \approx 2x^{-1/2}$ for $x \lesssim 1$.

To obtain an estimate for $\tilde{\epsilon}$ we can multiply the average attractive interaction

$$4\pi \int_{\sigma}^{\infty} V(r) r^2 dr = \frac{-32\pi}{9} \epsilon\sigma^3$$

by the maximum magnitude of the Gaussian weighted by e^{-2}. Thus

$$\tilde{\epsilon} \approx -\frac{32\pi}{9} \epsilon\sigma^3 \left(\frac{\alpha}{\pi}\right)^{3/2} e^{-2}$$

or

$$\tilde{\epsilon}/\epsilon \approx x^{3/2}/3.65 \tag{2.5}$$

for $x \lesssim 1$. In actual fact we obtain better agreement with experimental results for T_c^* if we replace 3.65 by $5^{3/4} = 3.34$ in the above equation. We shall make this replacement in our final expression for $\tilde{\epsilon}/\epsilon$.

Finally, since the distance from the hard core to the minimum of $V(r)$ is of order $(2^{1/6}-1)\sigma$, we expect that the asymptotic series of Eqs. (2.3) and (2.4) is valid for $2\alpha^{-1/2} \lesssim (2^{1/6}-1)\sigma$ or $\alpha\sigma^2 \gtrsim 250$. Taking the above results into account we arrive at our final expressions

$$\tilde{\epsilon}/\epsilon = [1 + 19.1x^{-1} + f(x)x^{-2}]^{-3/4}, \tag{2.6}$$

$$\tilde{\sigma}/\sigma = [1 + g(x)x^{-1}]^{1/2}, \tag{2.7}$$

where

$$f(x) = 5 + (177.7-5)[1 - \exp(-x/250)] \tag{2.8}$$

and

$$g(x) = 4 + (7.54-4)[1 - \exp(-x/250)]. \tag{2.9}$$

Equations (2.6) and (2.7) reduce to (2.3) and (2.4) as $x \to \infty$ and also give the expected x dependence, with corrected coefficients, for $x \lesssim 1$.

As mentioned in the Introduction, the above arguments leading to Eqs. (2.6) and (2.7) are lacking the mathematical rigor we would prefer. The physical arguments used do, however, appear to be plausible [except perhaps for the replacement $3.65 \to 5^{3/4}$ in Eq. (2.5) which, however, is still within our order of magnitude philosophy]. Rather than pursue this point further, we shall use Eqs. (2.6) and (2.7) to determine to what extent they correctly describe QM corrections to classical thermodynamic behavior.

III. VIRIAL COEFFICIENT, CRITICAL POINT, AND SURFACE TENSION

A. Second virial coefficient

The second virial coefficient for a classical gas interacting via the two-particle potential $V(r)$ is given by[13]

$$B(T) = -2\pi N \int_0^{\infty} [\exp -\beta V(r) - 1] r^2 dr, \tag{3.1}$$

where $\beta = (kT)^{-1}$. Using Eq. (2.1) this expression may be transformed to yield the reduced second virial coefficient $B^*(T^*)$, where

$$B^* = \frac{B(T)}{\frac{2}{3}\pi N\sigma^3} = 3\int_0^{\infty} [\exp -\beta^* f(x) - 1] x^2 dx, \tag{3.2}$$

$$f(x) = 4(x^{-12} - x^{-6}),$$

and $\beta^* = 1/T^*$. The function $B^*(T^*)$ has been tabu-

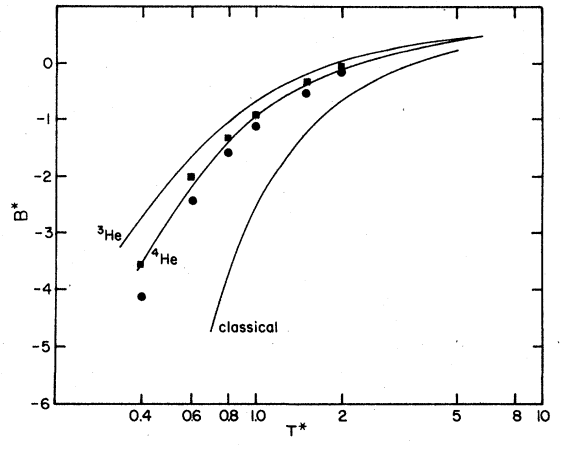

FIG. 2. Reduced second virial coefficient as a function of reduced temperature. The classical curve is given by Eq. (3.2). The curves for ^{3}He and ^{4}He are fully quantum-mechanical results from Ref. 18. The dots (^{4}He) and squares (^{3}He) are the results obtained using Eq. (3.3).

lated[13] and is shown in Fig. 2. In the absence of QM corrections all of the rare gases would be expected to have a $B^*(T^*)$ which lies along this curve. To compute the QM correction, we make the replacement $\epsilon \to \tilde{\epsilon}$ $\sigma \to \tilde{\sigma}$ in Eq. (3.1) to obtain $\tilde{B}(T)$. Dividing both sides of the resulting equation by $\frac{2}{3}\pi N\sigma^3$ we obtain the QM corrected expression

$$\tilde{B}^*(T^*) = \frac{\tilde{B}(T)}{\frac{2}{3}\pi N\sigma^3} = \left(\frac{\tilde{\sigma}}{\sigma}\right)^3 B^*\left(\frac{\epsilon}{\tilde{\epsilon}}\,T^*\right). \tag{3.3}$$

Thus, the QM corrections may be obtained by evaluating the classical result at a temperature scaled by $\epsilon/\tilde{\epsilon}$ and multiplying by $(\tilde{\sigma}/\sigma)^3$. The results of this operation, using Eqs. (2.6) and (2.7), are shown for ^{3}He and ^{4}He in Fig. 2. The smooth curves labeled ^{3}He and ^{4}He are the results of a fully QM calculation using Schrödinger's equation and appropriate phase-shift analysis.[18] As can be seen from Fig. 2 our results are in very good agreement with the "exact" calculation, e.g., at $T^*=1$ our approximation is capable of accounting for $\approx 90\%$ of the QM corrections to B^*.

B. Critical-point location

The variation of T_c^*, P_c^*, and V_c^* may easily be determined by combining corresponding-states theory with the results of Sec. II. For a purely classical system we would expect (Table I)

$$T_c^* = \frac{kT_c}{\epsilon} = 1.26, \tag{3.4a}$$

$$V_c^* = \frac{V_c}{N\sigma^3} = 3.1, \tag{3.4b}$$

$$P_c^* = \frac{P_c\sigma^3}{\epsilon} = 0.117, \tag{3.4c}$$

for all systems interacting via a 6-12 potential. The variation of the critical point with λ is obtained from Eqs. (3.4) by making the replacement $\epsilon \to \tilde{\epsilon}$, $\sigma \to \tilde{\sigma}$ to obtain

$$kT_c/\tilde{\epsilon} = 1.26$$

or

$$T_c^* = 1.26\tilde{\epsilon}/\epsilon, \tag{3.5a}$$

and

$$V_c^* = 3.1(\tilde{\sigma}/\sigma)^3, \tag{3.5b}$$

$$P_c^* = 0.117(\tilde{\epsilon}/\epsilon)(\sigma/\tilde{\sigma})^3. \tag{3.5c}$$

Equation (3.5a) may be solved graphically as shown in Fig. 3 where we have plotted the functions T_c^* and $1.26\,\tilde{\epsilon}/\epsilon$. The intercept of these curves yields T_c^* as a function of λ. This intercept, together with experimental values, is shown as a function of λ in Fig. 4. Once we have obtained T_c^* vs λ we may also determine V_c^* and P_c^* using Eqs. (3.5b) and (3.5c). These results are also shown in Fig. 4 together with appropriate experimental values. The overall agreement between theory and experiment is clearly quite good, the chief deficiency being the too rapid increase of V_c^* as λ increases. An additional positive aspect of the above approach is that it predicts no liquid-gas critical point for spin-polarized atomic hydrogen ($\lambda \simeq 4.74$) and deuterium ($\lambda \simeq 3.35$). Such a transition is expected for spin-polarized tritium ($\lambda \simeq 2.74$). All of these predictions are consistent with more sophisticated first principle calculations.[19]

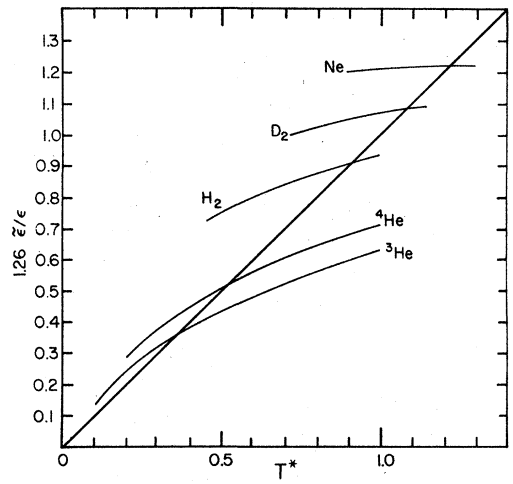

FIG. 3. Graphical solution for critical temperature using the equation $T^*=1.26\,\tilde{\epsilon}/\epsilon$.

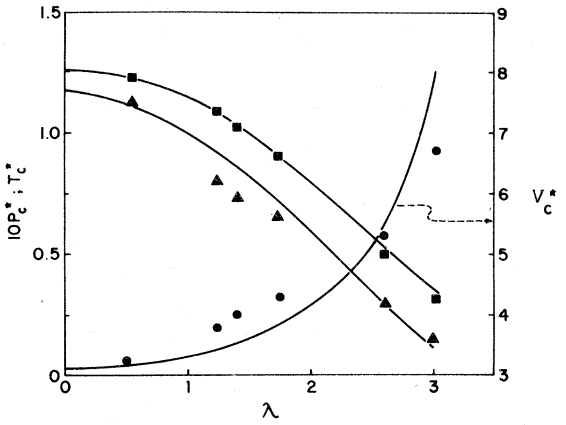

FIG. 4. Theoretical reduced critical-point volume, temperature, and pressure as a function of the quantum parameter λ. Experimental values are indicated by the data points [■ (T_c^*), ▲ (P_c^*), and ● (V_c^*)].

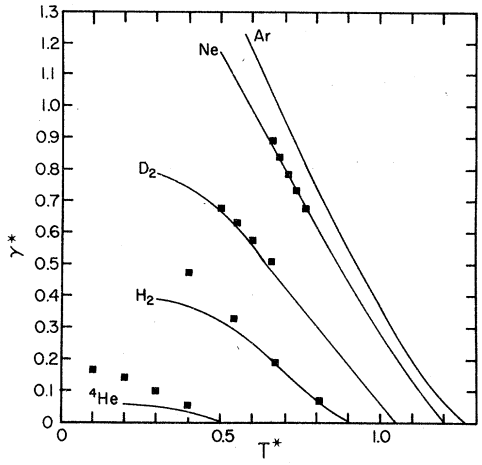

FIG. 5. Variation of reduced surface tension with reduced temperature. The curve for Ar is given by Eq. (3.6); all other curves are obtained from Eq. (3.7).

C. Surface tension

As an application of our theory to thermodynamic properties below T_c^* we shall consider the problem of QM corrections to the surface tension along the liquid-gas phase boundary, since to our knowledge this problem is largely unsolved. The approach is the same as before in that we assume that the experimental behavior of the heavier rare gases may be understood by some appropriate classical calculation using a potential of the form given by Eq. (2.1).[20] Thus we take the reduced surface tension of a classical 6-12 fluid to be given by

$$\gamma^* = \gamma\sigma^2/\epsilon = 2.666(1 - T^*/T_c^*)^{1.27}. \tag{3.6}$$

Setting $T_c^* = 1.26$ and making the standard replacements for ϵ and σ yields for the QM corrected surface tension

$$\tilde{\gamma}^* = \frac{\tilde{\gamma}\tilde{\sigma}^2}{\epsilon} = (\sigma/\tilde{\sigma})^2(\bar{\epsilon}/\epsilon)2.66\left(1 - \frac{T^*}{1.26\bar{\epsilon}/\epsilon}\right)^{1.27}. \tag{3.7}$$

In Fig. 5 we show the predicted variation of $\tilde{\gamma}^*$ with respect to T^* for Ne, D_2, H_2, and ^4He together with appropriate experimental results.[21-23] The qualitative agreement with experiment is excellent. Of particular interest is that our theory correctly predicts the bending of $\tilde{\gamma}^*$ toward the T^* axis as T^* decreases from T_c^*; the bending becoming more apparent as λ increases. This behavior is a result of both the decrease of $(\sigma/\tilde{\sigma})$ and the increased bending of $1.26\bar{\epsilon}/\epsilon$ toward the function T^* for $T^* < T_c^*$ (Fig. 3). This provides additional evidence that the T^* and λ dependence of $\bar{\epsilon}/\epsilon$ and $\tilde{\sigma}/\sigma$ is of real physical significance and that Eqs. (2.6) and (2.7) represent more than an *ad hoc* interpolation scheme.

IV. LIQUID-GAS COEXISTENCE CURVE

In this section we first apply the theory to an analysis of the global behavior of the liquid-gas coexistence curve and then proceed to a more detailed analysis near the liquid-gas critical point.

A. Global behavior

In determining the QM effects on the global properties of the coexistence curve we shall assume that the behavior of a purely classical fluid may be described by[24]

$$V_c^*/V_l^* = 1 + \tfrac{3}{4}(1 - T^*/T_c^*) + \tfrac{7}{4}(1 - T^*/T_c^*)^{1/3}, \tag{4.1}$$

$$V_c^*/V_g^* = 1 + \tfrac{3}{4}(1 - T^*/T_c^*) - \tfrac{7}{4}(1 - T^*/T_c^*)^{1/3}, \tag{4.2}$$

where V_l^*, V_g^*, and V_c^* are the reduced liquid, gas, and critical molar volume. These equations, while needing modification near the critical point, are sufficiently accurate for our study of the global properties.

A quantity of particular significance for our study is the rectilinear diameter defined by

$$d = \frac{1}{2}\left(\frac{V_c^*}{V_l^*} + \frac{V^*}{V_g^*}\right) = 1 + \tfrac{3}{4}(1 - T^*/T_c^*). \tag{4.3}$$

Scaling arguments[25] indicate that the $(1 - T^*/T^*)$ term is expected to have a singular behavior near the critical point, but again, the experimental data for classical gases may be fit quite nicely by a linear expression.[24,26] The curve labeled "classical" in Fig. 6 shows the behavior of Eqs. (4.1) and (4.2) for $T^*/T_c^* \leq 1$.

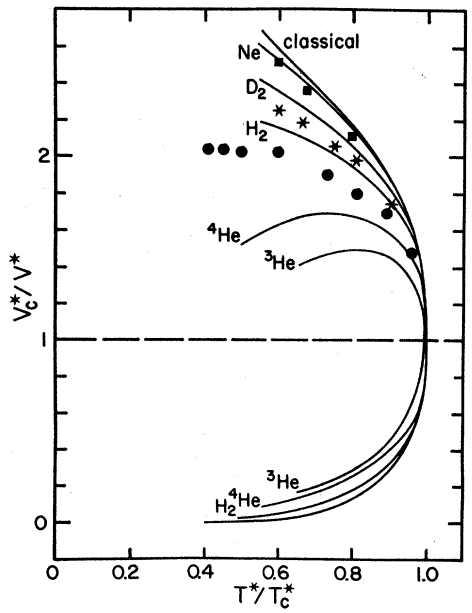

FIG. 6. Liquid-gas coexistence curves computed for the classical case [Eqs. (4.1) and (4.2)] and including quantum-mechanical corrections [Eqs. (4.6) and (4.7)]. Experimental points are for Ne (■), H_2 (*), and ^{4}He (●).

To determine the QM corrections to the above equations we use the fact that $V_c^*=3.1$ and $T_c^*=1.26$. Thus, under the replacement $\epsilon \to \tilde{\epsilon}$ we find

$$1-\frac{T^*}{T_c^*}=1-\frac{T^*}{1.26}\to 1-\frac{T^*}{1.26\tilde{\epsilon}/\epsilon}, \tag{4.4}$$

while

$$\frac{V_c^*}{V^*}=\frac{3.1}{V^*}\to\frac{3.1(\tilde{\sigma}/\sigma)^3}{V^*}=\frac{V_c^*(\tilde{\sigma}/\tilde{\sigma}_c)^3}{V^*}, \tag{4.5}$$

where $\tilde{\sigma}_c$ is the value of $\tilde{\sigma}$ at $T^*=T_c^*$. Making the appropriate substitution in Eqs. (4.1), (4.2), and (4.3) yields the following expressions:

$$\frac{V_c^*}{V_l^*}=\left(\frac{\tilde{\sigma}_c}{\tilde{\sigma}}\right)^3\left[1+\tfrac{3}{4}\left(1-\frac{T^*\epsilon}{1.26\tilde{\epsilon}}\right)+\frac{7}{4}\left(1-\frac{T^*\epsilon}{1.26\tilde{\epsilon}}\right)^{1/3}\right], \tag{4.6}$$

$$\frac{V_c^*}{V_g^*}=\left(\frac{\tilde{\sigma}_c}{\tilde{\sigma}}\right)^3\left[1+\frac{3}{4}\left(1-\frac{T^*\epsilon}{1.26\tilde{\epsilon}}\right)-\frac{7}{4}\left(1-\frac{T^*\epsilon}{1.26\tilde{\epsilon}}\right)^{1/3}\right], \tag{4.7}$$

and

$$d=\left(\frac{\tilde{\sigma}_c}{\tilde{\sigma}}\right)^3\left[1+\frac{3}{4}\left(1-\frac{T^*\epsilon}{1.26\tilde{\epsilon}}\right)\right]. \tag{4.8}$$

In Fig. 6 we show Eqs. (4.6) and (4.7) for Ne, D_2, H_2, ^{4}He, and ^{3}He together with selected experimental data[21,24] for Ne, H_2, and ^{4}He. The qualitative agreement is quite good and we get good quantitative agreement for H_2, D_2, and Ne. The behavior of the curves for ^{3}He for $T^*/T_c^*<0.8$ indicates a breakdown of our approximate expressions for $\tilde{\epsilon}/\epsilon$ and $\tilde{\sigma}/\sigma$. This anomalous behavior is primarily due to the too rapid increase of $\tilde{\sigma}/\sigma$ with decreasing temperature.

In spite of the above shortcomings, our results yield considerable insight as to the effect of QM corrections on the coexistence curve. In particular it has long been a puzzle as to why the helium liquids, where QM effects are most important, have a symmetrical coexistence curve similar to that of the classical lattice-gas model, which contains no QM effects and yields a perfectly symmetric coexistence curve.[27] Our results indicate that this similarity is quite fortuitous in that the QM effects suppress the intrinsic asymmetry of the classical curve to yield a nearly summetric coexistence curve. A quantitative measure of the

TABLE I. Molecular parameters for corresponding states reduction.[a]

	ϵ/k	σ	M	λ	T_c^*	$10P_c^*$	V_c^*	$P_c^*V_c^*/T_c^*$
^{3}He[b]	10.22	2.62	3.02	3.01	0.324	0.146	6.7	0.302
^{4}He[b]	10.22	2.62	4.00	2.61	0.51	0.29	5.31	0.302
H_2[c]	37	2.93	2.00	1.73	0.9	0.646	4.42	0.317
HD[c]	37	2.93	3.00	1.41	1.03	0.73	4.1	0.290
D_2[c]	37	2.93	4.00	1.22	1.1	0.86	3.9	0.305
Ne[d]	36.7	2.79	20.2	0.577	1.21	1.14	3.20	0.301
Ar[e]	120	3.41	40	0.187	1.25	1.16	3.12	0.289
Kr[e]	166.4	3.65	83.3	0.102	1.26	1.17	3.10	0.288

[a] Units are K for ϵ/k, Å for σ, and gm/mole for M.
[b] Reference 10.
[c] Reference 11.
[d] Reference 12.
[e] Reference 1.

TABLE II. Quantum-mechanical corrections to the rectilinear diameter for Lennard-Jones liquids.

	$a_1T_c^*$	$a_2T_c^*$	s_{theory}	s_{exp}
Xe	$<10^{-3}$	$>-10^{-3}$	0.75	0.75 [a]
Ar	$<10^{-2}$	$>-10^{-2}$	0.75	0.75 [a]
Ne	0.025	−0.02	0.71	0.72 [b]
D_2	0.14	−0.07	0.58	
HD	0.185	−0.091	0.52	
H_2	0.27	−0.15	0.4	0.37 [c]
^{4}He	0.53	−0.45	−0.11	0.18 [c] 0.05
^{3}He	0.64	−0.7	−0.43	−0.03 [c] −0.01

[a] Reference 24.
[b] Reference 26.
[c] Reference 28.

degree of symmetry is the slope s of the rectilinear diameter where s is defined by

$$d = 1 + s(1 - T^*/T_c^*) \ . \tag{4.9}$$

A purely classical liquid would be expected to have $s = 3/4$ [Eq. (4.3)]. Experimental values of s, for liquids where QM corrections are significant, are listed in Table II.[24,26,28] Although Eqs. (4.6) and (4.7) no longer yield a strictly linear rectilinear diameter, we can still define a theoretical expression for s by expanding Eq. (4.8) about $T^* = T_c^*$. Writing

$$1.26\tilde{\epsilon}/\epsilon = T_c^*[1 + a_1(T^* - T_c^*) \cdots] \ , \tag{4.10}$$

$$3.1(\tilde{\sigma}/\sigma)^3 = V_c^*[1 + a_2(T^* - T_c^*) \cdots] \ , \tag{4.11}$$

inserting these expansions in Eq. (4.8), and keeping only terms of order $1 - T^*/T_c^*$ yields

$$s = \tfrac{3}{4}(1 - a_1T_c^*) + a_2T^* \ . \tag{4.12}$$

In Table II, we list the values of $a_1T_c^*$ and $a_2T_c^*$ together with our values of s. The qualitative agreement is again quite good. From these results we also see that it is the large negative value of a_2T^* which causes our results to be too small for larger values of λ. This suggests that the primary reason for the breakdown of our theory at lower temperatures is the excessively rapid variation of $\tilde{\sigma}/\sigma$ with T^*.

B. Local critical-point behavior

The effects of QM corrections to the critical-point behavior of the liquid-gas system were first studied quantitatively by Fisher.[29] Since that early work there has been little development of the theory, primarily because there was no quantitative theory for the classical system. The recent advent of such a theory[11] allows us to re-examine the question of QM corrections in an almost trivial fashion.

Our approach will once again assume that the classical problem has been solved and that corresponding-states theory is valid. Since it is not our purpose to analyze the success of the classical theory,[30] we shall choose "typical" values for our classical critical-point exponents. The theory is sufficiently simple that should different exponents be desired the calculations that follow may be readily repeated.

It is convenient to consider the reduced fluid density and compressibility near the critical point of a classical 6-12 fluid to be given by[12,30]

$$\frac{V_c^*}{V^*} - 1 = B_0(1 - T^*/T_c^*)^{0.35} \ , \tag{4.13}$$

and

$$\rho^{*-1}\frac{\partial\rho^*}{\partial P^*} = K^* = \Gamma_0(1 - T^*/T_c^*)^{-1.21} \ . \tag{4.14}$$

If we perform the following steps: (i) Set $V_c^* = 3.1$ and $T_c^* = 1.26$ in Eqs. (4.13) and (4.14), (ii) take $T^* \to T^*(\epsilon/\tilde{\epsilon})$, $V^* \to V^*(\sigma/\tilde{\sigma})^3$, and $P^* \to P^*(\epsilon/\tilde{\epsilon})(\tilde{\sigma}/\sigma)^3$, (iii) use the series expansions (4.10) and (4.11), and (iv) keep only terms to the lowest order in $(1 - T^*/T_c^*) = t$, then Eqs. (4.13) and (4.14) become

$$\frac{V^*}{V^*} - 1 = B_0(1 - a_1T_c^*)^{0.35}t^{0.35} = \tilde{B}t^{0.35} \ , \tag{4.15}$$

and

$$K^* = \Gamma_0(1 - a_1T_c^*)^{-1.21}t^{-1.21} = \tilde{\Gamma}t^{-1.21} \ . \tag{4.16}$$

Equations (4.15) and (4.16) show that, within our model, there is no change in the critical exponents due to finite λ. The critical amplitudes are, however, significantly changed due to QM effects. In Fig. 7 we show the functions $(1 - a_1T^*)^{0.35}$ and $(1 - a_1T_c^*)^{-1.21}$ as a function of λ. Also shown are the experimental ratios[12] of the critical-point amplitudes $\tilde{B}/B_0$ and $\tilde{\Gamma}/\Gamma_0$ where we have taken $B_0 = 1.8$ and $\Gamma_0 = 0.06$. The agreement with experimental results is excellent. An interesting aspect of the above results is that only the derivative of $1.26\tilde{\epsilon}/\epsilon$ [Eq. (4.10)] enters into the correction for the critical-point amplitudes. This behavior is a result of the fact that Eqs. (4.13) and (4.14) are only singular functions of the temperature. The excellent agreement with experimental results thus confirms our previous contention that the weakest aspect of our model lies in the expression used for $\tilde{\sigma}/\sigma$.

The QM corrections to all other critical-point amplitudes may be readily obtained from the above results if we assume a "restricted cubic model" to represent the thermodynamic behavior of the

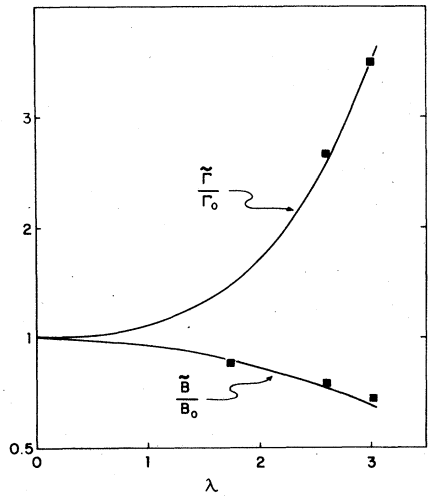

FIG. 7. Theoretical ratio of quantum-corrected critical-point amplitudes $(\tilde{B}, \tilde{\Gamma})$ to classical critical-point amplitudes (B_0, Γ_0) as a function of the quantum parameter λ. Experimental results are indicated by data points. Note the change of scale along the ordinate axis.

liquid-gas critical point.[30,31] This model contains two parameters a and k (not to be confused with Boltzmann's constant) which are adjusted for each substance and once determined permit the calculation of all critical-point amplitudes.[30,32] In particular the amplitudes B_0 and Γ_0 of Eqs. (4.13) and (4.14) are given by[32]

$$B_0 \approx 1.602k \quad \text{and} \quad \Gamma_0 = k/a \ . \tag{4.17}$$

Equation (4.17) may readily be inverted to obtain the QM corrections to k and a using Eqs. (4.15) and (4.16) and we find

$$\tilde{k} = k_0(1 - a_1 T_c^*)^{0.35} \ , \tag{4.18}$$

and

$$\tilde{a} = a_0(1 - a_1 T_c^*)^{1.56} \ . \tag{4.19}$$

In Fig. 8 we show the theoretical curves $k_0/\tilde{k}$ and $a_0/\tilde{a}$ together with the experimentally determined ratios[30] assuming the classical values $k_0 = 1.16$ and $a_0 = 14.2$. The agreement with experiment is good. The larger deviations for $a_0/\tilde{a}$ are in part due to the choice of $a_0 = 14.2$ which leads to a value of $\Gamma_0 = k_0/a_0 = 0.08$. If a_0 is increased so as to yield our assumed value[12] of $\Gamma_0 = 0.06$, the difference between theory and experiment is reduced but not eliminated. Further support for our theoretical value of $a_0/\tilde{a}$ may be found in the experimental results for the amplitude for the specific heat divergence near the critical point. If we define this amplitude above (+) and below (−) the critical temperature by $C_v^*/T^* = A_\pm |t|^{-\alpha}$ then the amplitudes $A_\pm$ are both proportional to ka in the restricted cubic model. Thus, our

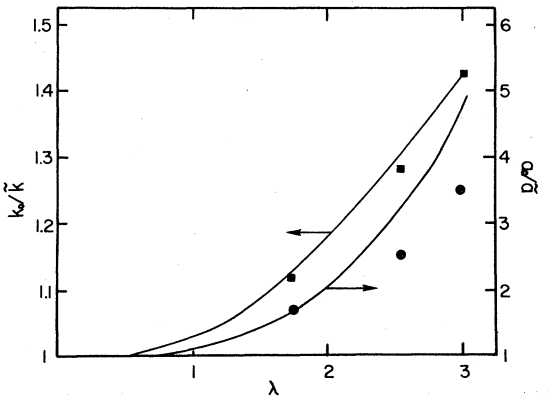

FIG. 8. Theoretical ratio of classical parameters (k_0, a_0) to quantum-corrected parameters $(\tilde{k}, \tilde{a})$ used in the restricted cubic model of critical-point behavior. Experimental values are indicated by data points and are taken from Ref. 30.

theory would predict

$$\frac{A_\pm}{\tilde{A}_\pm} = (1 - a_1 T_c^*)^{-1.91} \ .$$

In Table III we list our computed values of $A_\pm/\tilde{A}_\pm$, the experimental values[33] for ^{3}He and ^{4}He, and the values obtained using the parameters k and a listed in Ref. 30. We see that our computed ratios are in much better agreement with experiment than those obtained from the adjustable parameters[30] k and a.

Since the critical-point exponents were unaffected, it is worthwhile to extend the above analysis to include corrections-to-scaling terms[12,34,35] to determine how their singular behavior is affected. We thus replace Eqs. (4.13) and (4.14) with the more accurate expressions[12]

$$\frac{V_c^*}{V^*} - 1 = B_0 t^{0.32}[1 + b_0 t^{0.5} + O(t)] \ , \tag{4.20}$$

and

$$K^* = \Gamma_0 t^{-1.24}[1 + \gamma_0 t^{0.5} + O(t)] \ . \tag{4.21}$$

Repeating the procedure described above we

TABLE III. Quantum-mechanical corrections for the specific heat divergence amplitude at the critical point.

	Experimental[a] values		Present theory	Restricted cubic model[b]
	$A_+/\tilde{A}_+$	$A_-/\tilde{A}_-$	$A_\pm/\tilde{A}_\pm$	$A_\pm/\tilde{A}_\pm$
^{4}He	4.15	4.02	4.23	3.03
^{3}He	10.17	5.07	7.04	4.64

[a] Reference 32. We have used the values obtained for Xe for the classical values $A_\pm$.

[b] Reference 30.

arrive at QM corrected expressions of the form

$$\frac{V_c^*}{V^*} - 1 = B_0(1 - a_1 T_c^*)^{0.32} t^{0.32}[1 + b_0(1 - a_1 T_c^*)^{0.5} t^{0.5} + b_1 t^{0.68} + O(t)] \quad (4.22)$$

and

$$K^* = \Gamma_0(1 - a_1 T_c^*)^{-1.24} t^{-1.24}[1 + \gamma_0(1 - a_1 T_c^*)^{0.5} \times t^{0.5} + O(t)] , \quad (4.23)$$

where

$$b_1 = \frac{a_2 T_c^*}{B_0(1 - a_1 T_c^*)^{0.32}} . \quad (4.24)$$

The $b_1 t^{0.68}$ term in Eq. (4.22) changes sign with B_0 and represents one of the previously discussed correction terms ($a_2 T_c^*$) to the "rectilinear diameter". Our analysis thus implies that no corrections-to-scaling terms appear as a consequence of QM effects and the amplitude ratio b_0/γ_0 is unaffected by QM corrections. The correction amplitudes themselves do, however, undergo significant change due to QM effects and as Eqs. (4.22) and (4.23) show these amplitudes should increase as we go toward more classical fluids. In this connection it is worth noting that in the case of γ_0 this behavior is *opposite* to the predicted (and observed) behavior of Γ_0. Confirmation of these trends in the correction amplitudes and evidence of the $(1 - a_1 T_c^*)^{0.5}$ factor would provide a significant additional test of the theory.

V. SOLID PHASE PROPERTIES

In this section we apply our theory to the properties of the rare gases along the solid-liquid melting curve and to the dynamical properties of the solid phase at high temperature. Crawford[26] has given an excellent review of this topic and we shall make use of his collection and parametrization of experimental data in our analysis.

A. Thermodynamic properties along the melting curve

We represent the melting pressure data by the empirical modified Simon equation[26] which may be written in the form

$$P = A(T - T_0)^c - B . \quad (5.1)$$

Choosing argon as our classical standard[26] and using the parameters listed in Table I we may write a reduced melting equation for the classical 6-12 fluid as

$$P^* = A^*(T^* - T_0^*)^c - B^* , \quad (5.2)$$

where $A^* = 11.24$, $B^* = 3.54$, $T_0^* = 0.25$, and $c = 1.43$. Making the standard replacements we obtain the following expression for P^* when QM corrections are important:

$$\tilde{P}^* = \left(\frac{\sigma}{\tilde{\sigma}}\right)^3 \left[A^* \left(T^* \frac{\epsilon}{\tilde{\epsilon}} - T_0^* \right)^c - B^* \right] . \quad (5.3)$$

In Fig. 9(a) we show Eq. (5.2), which gives a good representation of the Ar, Kr, and Xe data, together with Eq. (5.3) and selected experimental values of P^* for ^{3}He and ^{4}He. We can see that Eq. (5.3) provides a rather good description of the QM effects on the behavior of P^* vs T^*.

Another quantity which shows significant λ dependence is the change in volume upon melting. Again, using argon as our classical fluid,[26] we can write for the reduced change in volume

$$\Delta V^* = D^*/(T^* - T_1^*)^d , \quad (5.4)$$

where ΔV^* is the difference in molar volumes for the fluid and solid $D^* = 0.0658$, $T_1^* = 0.494$, and $d = 0.527$. The corresponding equation, including QM corrections is

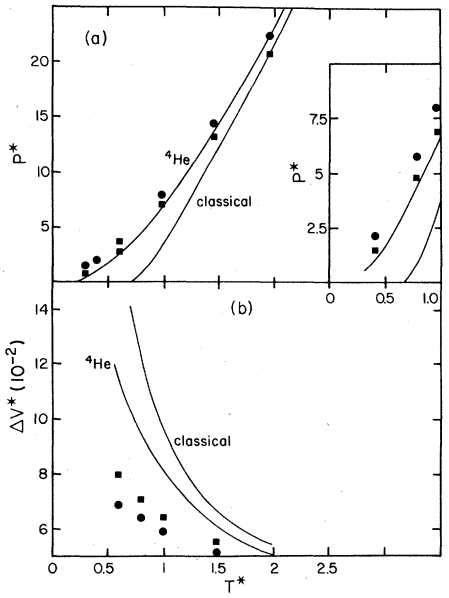

FIG. 9. (a) Reduced pressure versus reduced temperature along the solid-liquid melting line. The classical curve is obtained from Eq. (5.2), the ^{4}He curve from Eq. (5.3), the curve for ^{3}He lies above that of ^{4}He, but is indistinguishable from ^{4}He on this scale. Experimental points (■ = ^{4}He, ● = ^{3}He) are from Ref. 26. (b) Change in reduced molar volume upon melting. The classical curve is obtained from Eq. (5.4), the ^{4}He curve from Eq. (5.5). The curve for ^{3}He is indistinguishable from ^{4}He on this scale.

$$\Delta\tilde{V}^* = \left(\frac{\tilde{\sigma}}{\sigma}\right)^3 D^* \Big/ \left[T^* \frac{\epsilon}{\tilde{\epsilon}} - T_1^*\right]^d . \qquad (5.5)$$

Figure 9(b) shows Eqs. (5.4) and (5.5) for ^{3}He and ^{4}He together with the experimental results.[26] These curves together with those of Fig. 9(a) show that the present theory provides a qualitative account for QM effects along the melting curve. The rather too large value of $\tilde{\sigma}/\sigma$ is the principal reason for the depression of the computed $\tilde{P}^*$ and elevation of $\Delta\tilde{V}^*$ with respect to the experimental results.

B. Debye temperature at melting

To determine the applicability of our theory to dynamic quantities we analyze the QM corrections to the Debye temperature at the melting point (θ_∞) of ^{3}He and ^{4}He. Since many different approximations to $\tilde{V}(r)$ may yield similar thermodynamic behavior, an analysis of θ_∞, which depends on the second derivative of $\tilde{V}(r)$, provides a significant additional test of our approximations. For our classical model we use the result of Domb *et al.*[36,37] for the value of θ_∞ for a classical solid in the limit of high temperature ($T \gtrsim \theta_D/5$). In our notation we have

$$\theta_\infty = 0.29 \frac{h}{k\sqrt{m}} \left(\frac{d^2V}{dr^2}\right)^{1/2} , \qquad (5.6)$$

where we have assumed an fcc lattice with nearest-neighbor interactions and a two-body potential given by Eq. (2.1). By making the replacement $\epsilon \to \tilde{\epsilon}$ and $\sigma \to \tilde{\sigma}$ we obtain the following QM corrected expression for θ_∞:

$$\theta_\infty = 0.895 \frac{\lambda\epsilon}{k} \left(\frac{\tilde{\epsilon}}{\epsilon}\right)^{1/2} \left(\frac{\tilde{\sigma}}{\sigma}\right)^3 \frac{1}{V^{*4/3}} \left[\frac{13}{V^{*2}} \left(\frac{\tilde{\sigma}}{\sigma}\right)^6 - 1\right]^{1/2} , \qquad (5.7)$$

where $V^* = V/10.88$ and V is the molar volume. In Fig. 10 we show Eqs. (5.6) and (5.7) for ^{3}He and ^{4}He together with some experimental results.[37-39] The theory is in qualitative agreement with experiment at the smaller molar volumes. Our expressions for $\tilde{\sigma}/\sigma$ and $\tilde{\epsilon}/\epsilon$ are presumably more reliable in this region due to the higher melting temperatures. An additional aspect of our results is that, in spite of the large increase in θ_∞ due to QM effects, the ratios of θ_∞ for ^{3}He to that of ^{4}He obtained from Eq. (5.7), at the same molar volume, are very close to the classical value of $(\frac{4}{3})^{1/2} = 1.155$. In particular, for molar volumes ranging from 10.5 to 14 cm^3 we find that the ratios of Debye temperatures range from 1.21 to 1.32, whereas the experimental results have a ratio ≈ 1.22. This behavior is also consistent with that observed by Ahlers[38] for the same ratio taken at $T = 0$.

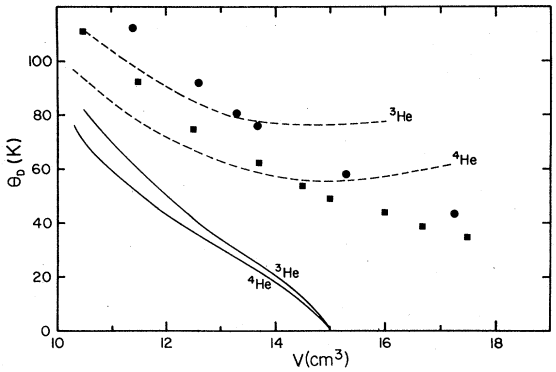

FIG. 10. Variation of Debye temperature with molar volume along the melting curve. The solid curves are the classical results obtained from Eq. (5.6). The dashed curves are obtained from Eq. (5.7) and include quantum corrections. Experimental values (■=^{4}He, ● = ^{3}He) are taken from Refs. 36, 37, and 38.

VI. SUMMARY AND CONCLUSIONS

By utilizing the theory of corresponding states together with Feynman's method of including QM effects via a temperature-dependent effective potential, we have been able to provide an excellent qualitative, and frequently quantitative, account of the influence of QM effects on the thermal properties of Lennard-Jones fluids. In particular the theory is able to account for the following:

(a) QM corrections to the second virial coefficient.

(b) The dependence of the critical-point location (T_c, V_c, P_c) on the quantum parameter λ.

(c) The change in shape of the liquid-gas and solid-liquid coexistence curves as λ increases.

(d) The decrease in the slope of the rectilinear diameter as λ increases.

(e) The dependence of critical point amplitudes on λ.

(f) The quantum-mechanical enhancement of the Debye temperature near the solid melting point. In addition, the theory predicts the λ dependence of the correction-to-scaling amplitudes near the liquid-gas critical point, with all of these amplitudes expected to be larger for classical liquids and to decrease as λ increases.

In spite of all these successes there remains an essential difficulty with our approach, namely, the absence of a mathematically well-defined procedure for computing an effective potential when there is a strong hard-core-type singularity at the origin of the two-body potential. We have

used physical arguments to circumvent this problem and the results obtained provide *aposteriori* evidence that our approach contains a large element of truth. There are doubtless many other ways of defining $\tilde{\epsilon}/\epsilon$ and $\tilde{\sigma}/\sigma$ which would give even better agreement with experiment than we have achieved. We have frankly not made an effort to search for optimum expressions [except for the choice of "5" in Eq. (2.8)], since our philosophy was to rely as much as possible on physical arguments and avoid curve fitting. The success of our approach indicates that *an effective temperature-dependent potential which includes QM effects does exist*, and efforts toward extending Feynman's theory to include singular potentials would be well rewarded.

ACKNOWLEDGMENT

This work was supported in part by the Theoretical Physics Division of the Arizona Research Laboratories.

APPENDIX A: DERIVATION OF EFFECTIVE POTENTIAL APPROXIMATION

The N-particle partition function, in the absence of exchange effects, is given by the path integral expression[17]

$$Z=\frac{1}{N!}\int d^N\vec{\mathrm{P}}(0)\int_{\vec{\mathrm{R}}_i(0)}^{\vec{\mathrm{R}}_i(0)}\exp-\frac{1}{2\hbar}\left(\int_0^{\beta\hbar} m\sum_i\dot{\vec{\mathrm{R}}}_i^2\,dt+\sum_{ij}V(\vec{\mathrm{R}}_i-\vec{\mathrm{R}}_j)dt\right)D^N\vec{\mathrm{R}}(t)\ , \tag{A1}$$

where the $\sum_i$ runs over all particles, $V(\vec{\mathrm{R}}_i-\vec{\mathrm{R}}_j)$ is the assumed two-particle potential, and $\beta=1/kT$. Assuming a potential of the form given by Eq. (2.1) and introducing the dimensionless quantities

$$\begin{aligned}
&\vec{\mathrm{X}}=\vec{\mathrm{R}}/\sigma\ ,\\
&V(\vec{\mathrm{R}}_i-\vec{\mathrm{R}}_j)/\epsilon=U(\vec{\mathrm{X}}_i-\vec{\mathrm{X}}_j)=U_{ij}\ ,\\
&t=\sigma(m/\epsilon)^{1/2}\tau\ ,\\
&\tilde{\hbar}=\hbar/(m\epsilon\sigma^2)^{1/2}\ ,\\
&\tilde{\beta}=\epsilon/kT\ .
\end{aligned} \tag{A2}$$

Equation (A1) may be written as

$$Z=\frac{1}{N!}\int d^N\vec{\mathrm{X}}\int_{\mathrm{X}(0)}^{\mathrm{X}(0)}\exp-\frac{1}{2\tilde{\hbar}^2}\left(\int_0^{\tilde{\beta}\tilde{\hbar}}\sum_i|\dot{\vec{\mathrm{X}}}_i|^2d\tau+\sum_{ij}U_{ij}\,d\tau\right)D^N\vec{\mathrm{X}}(\tau)\ . \tag{A3}$$

Introducing the weight function

$$W=\frac{\exp\left(-\frac{1}{2\tilde{\hbar}}\int_0^{\tilde{\beta}\tilde{\hbar}}\sum_i|\dot{\vec{\mathrm{X}}}_i|^2d\tau\right)}{\int_{\mathrm{X}_i(0)}^{\mathrm{X}_i(0)}\exp\left(-\frac{1}{2\tilde{\hbar}}\int_0^{\tilde{\beta}\tilde{\hbar}}\sum_i|\dot{\vec{\mathrm{X}}}_i|^2d\tau\right)D^N X}\ ,$$

the "average" position

$$\bar{X}_i=\frac{1}{\tilde{\beta}\tilde{\hbar}}\int_0^{\tilde{\beta}\tilde{\hbar}}\vec{\mathrm{X}}_i(\tau)d\tau\ ,$$

and $f_{ij}=(U_{ij}-\bar{U}_{ij})$, where $\bar{U}_{ij}=U(\bar{X}_i-\bar{X}_j)$, we can write Eq. (A3) as

$$Z=\frac{D}{N!}\int d^N\vec{\mathrm{X}}(0)\exp\left(-\frac{\tilde{\beta}}{2}\sum_{ij}\bar{U}_{ij}\right)\int_{\mathrm{X}(0)}^{\mathrm{X}(0)}W(X_i)\exp\left(-\frac{1}{2\tilde{\hbar}}\int_0^{\tilde{\beta}\tilde{\hbar}}\sum_{ij}(U_{ij}-\bar{U}_{ij})d\tau\right)D\vec{\mathrm{X}}^N(\tau)\ , \tag{A4}$$

where D is the denominator in the expression for W. We now let $\int d^N\vec{\mathrm{X}}(0)\to\int d^N\bar{X}$ and redefine the path

integral in Eq. (A4) to be evaluated with $\bar{X}$ held constant and with an integration over the end points $\vec{X}(0)$. The path integral term in Eq. (A4) is of the form $\langle e^g \rangle$, where $\langle g \rangle \rightarrow \int W g D^N X$ and

$$g = -\frac{1}{2\tilde{\hbar}} \int \sum_{ij} f_{ij} \, d\tau \ .$$

Using the result[17] that

$$\langle e^g \rangle \geq e^{\langle g \rangle} \ ,$$

we can get an upper limit on the free energy by using the approximation

$$Z \geq \frac{1}{N!} \int d\vec{\bar{X}} \, D \exp\left(-\frac{\tilde{\beta}}{2} \sum_{ij} \bar{U}_{ij} \right) e^{\langle g \rangle} \ . \tag{A5}$$

Using the definition of $\langle g \rangle$ it is easy to see that $\langle g \rangle$ involves the sum of two-body path integrals of the form

$$W_{1,2} = \frac{\frac{1}{2\tilde{\hbar}} \int \int_0^{\tilde{\beta}\tilde{\hbar}} f_{1,2} d\tau \exp\left(-\frac{1}{2\tilde{\hbar}} \int_0^{\tilde{\beta}\tilde{\hbar}} (|\dot{\vec{X}}_1|^2 + |\dot{\vec{X}}_2|^2) d\tau \right) D\vec{X}_1 D\vec{X}_2}{\int \int \exp - \frac{1}{2\tilde{\hbar}} \int_0^{\tilde{\beta}\tilde{\hbar}} (|\dot{\vec{X}}_1|^2 + |\dot{\vec{X}}_2|^2) D X_1 D X_2} \ , \tag{A6}$$

where the paths are to be taken with $\vec{\bar{X}}_1$ and $\vec{\bar{X}}_2$ fixed and we integrate over starting points $\vec{X}(0)$.

The change of variables

$$\vec{y} = \vec{X}_1 - \vec{X}_2 \ ,$$
$$\vec{z} = \vec{X}_1 + \vec{X}_2 \ ,$$

reduces $W_{1,2}$ to the one-body path integral evaluated by Feynman.[17] Substituting the result in Eq. (A5) yields an approximate expression for Z given by

$$Z \geq \frac{D}{N!} \int d\vec{r}_1 \cdots d\vec{r}_N \exp\left(-\frac{\beta}{2} \sum_{ij} \tilde{V}(|\vec{r}_i - \vec{r}_j|) \right) \ . \tag{A7}$$

Equation (A7) is of the same form as the partition function for a purely classical system with the interaction between particles now being given by the effective potential $\tilde{V}(r)$ rather than the bare potential $V(r)$.

APPENDIX B: DERIVATION OF EQUATIONS (2.3) AND (2.4)

Expanding $V(r)/\epsilon$ in a power series in $|\vec{r}| - r_0 (r_0 = 2^{1/2}\sigma)$ yields

$$V(r)/\epsilon = 1 + \tfrac{1}{2} K(|\vec{r}| - r_0)^2 + \tfrac{1}{6} L(|\vec{r}| - r_0)^3 + \tfrac{1}{24} M(|\vec{r}| - r_0)^4 \ . \tag{B1}$$

Inserting (B1) in Eq. (2.2) results in integrals of the form

$$\left(\frac{\alpha}{\pi}\right)^{3/2} \int |\vec{r}'|^n e^{-\alpha |(\vec{r} - \vec{r}')|^2} d^3\vec{r}' \ . \tag{B2}$$

For n even it is convenient to write (B2) in Cartesian coordinates, choosing $\vec{r}$ to lie along the z axis we obtain

$$\left(\frac{\alpha}{\pi}\right)^{3/2} \int_{-\alpha}^{+\alpha} \int \int (x'^2 + y'^2 + z'^2)^{n/2} e^{-\alpha(x'^2 + y'^2 + (z' - r)^2)} dx' \, dy' \, dz' \ . \tag{B3}$$

For n even, integrals of the above form may be evaluated exactly. For n odd it is more convenient to rewrite (B2) in spherical coordinates. Again taking r along the z axis and performing the angular integration results in integrals of the form

$$\left(\frac{\alpha}{\pi}\right)^{3/2} \left(\frac{\pi}{\alpha r}\right) \int_0^\infty x^{n+1} (e^{-\alpha(x - r)^2} - e^{-\alpha(x + r)^2}) dx \ . \tag{B4}$$

For $\alpha r^2 \gg 1$ and $n=1$ or 3 integrals like (B4) contain terms proportional to r^3, r, r^{-1}, and $e^{-\alpha r^2}$. We ignore terms proportional to $e^{-\alpha r^2}$ and expand those terms of order r^{-1} as

$$\frac{1}{r} = \frac{1}{r - r_0 + r_0} = \frac{1}{r_0}\left(1 - \frac{r - r_0}{r_0} + \frac{(r - r_0)^2}{r_0^2} - \cdots\right). \tag{B5}$$

Using this expansion together with the higher powers of r obtained in (B3) and (B4) yields an expression for $\tilde{V}(r)$ of the form

$$\frac{\tilde{V}(r)}{\epsilon} = C_0 - C_1(r - r_0) + \tfrac{1}{2} C_2 (r - r_0)^2 \cdots, \tag{B6}$$

where the constants C_0, C_1, and C_2 depend on K, L, M, r_0, and $\alpha\sigma^2$. The location of the minimum of (B6) is set equal to $2^{1/6}\tilde{\sigma}$ while the value at the minimum is set equal to $\tilde{\epsilon}/\epsilon$. The resulting expressions are given in Eqs. (2.3) and (2.4).

[1] J. de Boer, Physica (Utrecht) 14, 139 (1948).
[2] J. de Boer and B. S. Blaisse, Physica (Utrecht) 14, 149 (1948).
[3] J. de Boer and R. J. Lunbeck, Physica (Utrecht) 14, 520 (1948).
[4] John D. Rogers and F. G. Brickwedde, Physica (Utrecht) 32, 1001 (1966).
[5] Jean-Pierre Hansen and Jean Jacques Weis, Phys. Rev. 188, 314 (1969).
[6] T. Burke, J. L. Lebowitz, and E. Lieb, Phys. Rev. 149, 118 (1966).
[7] T. S. Nilsen and P. C. Hemmer, J. Stat. Phys. 1, 175 (1969).
[8] P. C. Hemmer and J. L. Lebowitz, in *Phase Transitions and Critical Phenomena* edited by C. Domb and M. S. Green (Academic, New York, 1976), V. 5b.
[9] L. H. Nasanow, L. J. Parish, and F. J. Pinski, Phys. Rev. B 11, 191 (1975).
[10] M. D. Miller, L. H. Nasanow, and L. J. Parish, Phys. Rev. Lett. 35, 581 (1975).
[11] K. G. Wilson and J. Kogut, Phys. Rep. 12C, 75 (1974).
[12] Charles Pittman, Theodore Doiron, and Horst Meyer, Phys. Rev. B 20, 3678 (1979).
[13] J. O. Hirschfelder, C. F. Curtiss, and R. B. Bird, *Molecular Theory of Gases and Liquids* (Wiley, New York, 1954).
[14] J. P. Hansen, Phys. Lett. 34A, 25 (1971).
[15] J. S. Brown, Phys. Lett. 29A, 121 (1969).
[16] J. A. Barker, in *Rare Gas Solids*, edited by M. L. Klein and J. A. Venables (Academic, New York, 1976), Vol. I.
[17] R. P. Feynman, *Statistical Mechanics* (Benjamin, Reading, Mass., 1972), p. 88–96.
[18] John E. Kilpatrick, William E. Keller, Edward F. Hammel, and Nicholas Metropolis, Phys. Rev. 94, 1103 (1954).
[19] R. D. Etters, J. V. Dugan, and R. W. Palmer, J. Chem. Phys. 62, 313 (1975).
[20] Frank P. Buff and R. A. Lovett, in *Simple Dense Fluids*, edited by H. L. Frisch and Z. W. Salisburg (Academic, New York, 1968).
[21] N. B. Vargaftik, *Tables on the Thermophysical Properties of Liquids and Gases* (Hemisphere, Washington, D.C., 1975).
[22] Dudley B. Chelton and Douglas B. Mann, *Cryogenic Data Book* (National Bureau of Standards, Cryogenic Engineering Laboratory, Boulder, Colorado); also available through University of California Radiation Laboratory Document No. 3421 (unpublished).
[23] J. Wilks, *The Properties of Liquid and Solid Helium* (Clarendon, Oxford, 1967), Chap. 14.
[24] E. A. Guggenheim, J. Chem. Phys. 13, 253 (1945).
[25] C. Vause and J. Sak, Phys. Rev. A 21, 2099 (1980).
[26] R. K. Crawford, *Rare Gas Solids*, edited by M. L. Klein and J. A. Venables (Academic, London, 1977), Vol. 2, Chap. 11.
[27] H. E. Stanley, *Introduction to Phase Transitions and Phenomena* (Oxford University Press, London, 1971).
[28] G. R. Brown and H. Meyer, Phys. Rev. A 6, 364 (1972).
[29] Michael E. Fisher, Phys. Rev. Lett. 16, 11 (1966).
[30] Jan V. Sengers and J. M. H. Levelt Sengers, *Progress in Liquid Physics*, edited by Clive A. Craxton (Wiley, New York, 1978).
[31] J. T. Ho and J. D. Lister, Phys. Rev. B 2, 4523 (1970).
[32] M. R. Moldover, J. V. Sengers, R. W. Gamman, and R. J. Hocken, Rev. Mod. Phys. 51, 79 (1979).
[33] G. Raymond Brown and Horst Meyer, Phys. Rev. A 6, 364 (1972).
[34] Amnon Aharony and Guenter Ahlers, Phys. Rev. Lett. 44, 785 (1980).
[35] Mau-Chung Chang and A. Houghton, Phys. Rev. Lett. 44, 785 (1980).
[36] C. Domb and L. S. Satter, Philos. Mag. 43, 1683 (1952).
[37] C. Domb and J. S. Dugdale, *Progress in Low Temperature Physics*, edited by C. J. Gorter (North-Holland, Amsterdam, 1957), Vol. 2.
[38] Guenter Ahlers, Phys. Rev. A 2, 1505 (1970).
[39] H. H. Sample and C. A. Swenson, Phys. Rev. 158, 188 (1967).